THE ASTRONOMICAL JOURNAL VOLUME 107, NUMBER 4 APRIL 1994

IONIZATION CONES AND RADIO EJECTA IN ACTIVE GALAXIES

A. S. WILSON

Space Telescope Science Institute, 3700 San Martin Drive, Baltimore, Maryland 21218 and Astronomy Department, University of Maryland, College Park, Maryland 20742
Electronic mail: awilson@stsci.edu

Z. I. TSVETANOV

Center for Astrophysical Sciences, Department of Physics and Astronomy, Johns Hopkins University, Baltimore, Maryland 21218
Electronic mail: ztsvetanov@pha.jhu.edu

Received 1993 October 26; revised 1993 December 10

ABSTRACT

We report radio mapping at three frequencies of the Seyfert 2 galaxy NGC 5252, which is known to exhibit a spectacular pair of "ionization cones" in optical emission-line images. The radio structure of the galaxy comprises an unresolved (<50 pc) source coincident with the optical nucleus, weak, narrow features extending ≃900 pc to north and south from the nucleus, and an unresolved radio source some 10 kpc from the nucleus. The inner parts of the extended radio structure and the off-nuclear source align well with the axis of the ionization cones. There are currently 11 Seyfert galaxies known to possess an ionization cone or a bi-cone; 8 of these galaxies also contain a linear (double, triple, or jet-like) nuclear radio structure. For this limited, incomplete sample, there is a tight alignment between cone and radio axes: the formal mean difference between the measured projections of these axes on the sky is only 6°, and the alignment may well be better than this at the location(s) closer to the nucleus where the collimation occurs. Although the *degree* of collimation is much worse for the ionizing photons than for the radio plasma, it is clear that they are collimated by the same, or coplanar, nuclear disks or tori. In particular, if the ionization cones result from absorption by dusty tori on the pc scale and the radio ejecta from accretion disks around the central black hole, the absence of differential precession indicates that either the gravitating mass distribution is close to spherical or the dusty torus has settled into a preferred plane. The cones currently known in late-type (but not early-type) spirals show a trend to align with the axis of the galaxy stellar disk. We argue that this alignment is either an observational selection effect or indicates that the gas accreted to power the nuclear activity has an internal origin in late-type spirals, but may have an external origin (e.g., a galaxy merger) in early-types.

1. INTRODUCTION

Recent work has indicated that the emission from the Narrow Line Regions (NLR's) of Seyfert galaxies is generally aligned with the radio axes. The NLR gas is found to be associated with the "linear" radio sources on the tens of pc to kpc scales (e.g., Haniff *et al.* 1988; Whittle *et al.* 1988). On a scale larger than the radio sources, emission-line gas is found which is kinematically little disturbed by the nuclear activity, but exhibits a high ionization spectrum characteristic of photoionization by the nonstellar nuclear source. This gas—termed the Extended Narrow Line Region (ENLR)—also tends to be aligned with the radio axis (Unger *et al.* 1987). Sometimes, the gas in the ENLR exhibits a conical or bi-conical shape, with the nucleus at the apex (e.g., Pogge 1989). This morphology is indicative of illumination of gas by a collimated source of ionizing radiation and provides important supporting evidence for so-called "Unified Models" of active galactic nuclei (e.g., Antonucci 1993).

The properties of the linear radio sources and the "ionization cones" provide valuable constraints on the nuclear disks or tori which are presumably responsible for their collimation. The relationship between these structures and the disk of the parent galaxy is also relevant to the origin of the nuclear disks. The present paper presents radio maps of a galaxy with ionization cones and discusses the general relationship between the radio sources, the ionization cones, and the disks of the host galaxies.

In Secs. 2 and 3, we report radio maps of the galaxy NGC 5252, which contains one of the most spectacular ionization bi-cones known (Tadhunter & Tsvetanov 1989). Section 4 reviews the cones currently known in Seyfert galaxies and shows that the projections of the cone and radio axes on the sky are very tightly aligned—often to within the errors of measurement. The relationship between the ionization cones and the disk of the host galaxies is also considered. The nature of the alignments and misalignments is briefly discussed in Sec. 5. Throughout this paper, we adopt $H_0=75$ km s^{-1} Mpc^{-1}, corresponding to a distance to NGC 5252 of 91.4 Mpc for the recession velocity (corrected to the "galactic standard of rest") of 6852 km s^{-1} (de Vaucouleurs *et al.* 1991).

2. NEW RADIO OBSERVATIONS OF NGC 5252

NGC 5252 was observed with the Very Large Array[1] in "A" configuration on 1990 April 29. Observations were

[1]The Very Large Array is a facility of the National Radio Astronomy Observatory, which is operated by Associated Universities Inc., under contract with the National Science Foundation.

 0004-6256/94/107(4)/1227/8/$0.90

TABLE 1. Radio positions, flux densities, and spectral indices in NGC 5252.

(1)	Nuclear source[1] (2)	Nuclear core source[1] (3)	Off-nuclear source (4)
$\alpha_r(1950.0)$[2]		$13^h\ 35^m\ 44.340^s \pm 0.013^s$	$13^h\ 35^m\ 44.111^s \pm 0.013^s$
$\delta_r(1950.0)$[2]		$+\ 04°\ 47'\ 47.19'' \pm 0.2''$	$+\ 04°\ 48'\ 09.03'' \pm 0.2''$
S(20 cm) (mJy)	15.2±0.7		3.2±0.2
S (6 cm) (mJy)	11.6±0.6	9.6±0.6	1.9±0.2
S (3.6 cm) (mJy)	7.8±0.5	6.7±0.5	1.4±0.2
α[3](20–6 cm)	0.22±0.1		0.43±0.1
α[3](6–3.6 cm)	0.78±0.15	0.70±0.3	0.60±0.3

Notes to TABLE 1

[1]"Nuclear Source" refers to all radio emission within 3″ of the nuclear radio peak, while the "Nuclear Core Source" is the unresolved source, presumably associated with the true nucleus, seen in the 6 and 3.6 cm maps.

[2]α_r and δ_r are the radio right ascension and declination. The position of the optical nucleus is [Argyle & Eldridge 1990, corrected by Argyle (1993) for a typographical error]: α_o (1950.0)$=13^h\ 35^m\ 44.349^s \pm 0.008^s$, $\delta_o(1950.0) = +04°\ 47'\ 47.08'' \pm 0.11''$, so $\alpha_r - \alpha_o = -0.1'' \pm 0.2''$ and $\delta_r - \delta_o = +0.1'' \pm 0.2''$.

[3]Spectral index, defined as $S \propto \nu^{-\alpha}$.

made at 20, 6, and 3.6 cm wavelength, and followed the traditional procedure of sandwiching an integration of some 10–15 min on the galaxy between two observations of a calibration source. The source 1351−018, which is some 8° away from NGC 5252, was used as the calibrator. Two independent, contiguous IF's, each with bandwidth 50 MHz, were used in each band, giving central frequencies of 1.4899, 4.8601, and 8.4399 GHz and total bandwidths of 100 MHz. The total integration times on NGC 5252 were approximately 3, 3.8, and 2.4 h at these three frequencies, respectively. Absolute flux densities were established by means of observations of 3C286. Analysis followed usual methods, including cleaning and self-calibration at each frequency.

In order to provide a check on the fluxes, a second set of VLA observations at 20 and 6 cm was kindly obtained by G. van Moorsel on 1993 April 11. NGC 5252 was observed for 16 min at each wavelength with the array in "B" configuration. The fluxes at the two epochs agree to about 10% at 20 cm and to about 5% at 6 cm, and their averages are reported in Table 1.

3. RADIO MORPHOLOGY OF NGC 5252

Figure 1 is a contour plot of the 20 cm map of NGC 5252, while Fig. 2(a) shows a simplified version of this plot superposed on the [O III] λ5007 emission-line image of Tadhunter & Tsvetanov (1989). Figure 3 shows the [O III] λ5007 image as a color plate, with Tadhunter & Tsvetanov's (1989) green continuum image shown as yellow contours and the 20 cm radio image as blue contours. The stronger (southern) radio source is resolved and its core coincides with the optical continuum nucleus to better than 0.2″=90 pc (Table 1). The images of Tadhunter & Tsvetanov (1989) show no shift bigger than ≈0.1″ in either coordinate between the optical line and optical continuum peaks so, in aligning the radio and optical maps in Figs. 2 and 3, the peaks were taken to correspond. A second radio source, which is unresolved at all three frequencies [FWHM size (3.6 cm) <0.1″], is found 22″ north (PA −8.9°) of the nucleus. As may be seen from Figs. 1 and 2, the off-nuclear source lies approximately along the extension of the nuclear one. Figure 2(b) gives contours of the radio map of the nuclear source at 6 cm on the [O III] image. The nuclear source comprises an unresolved (<0.1″) core plus weak, narrow features, suggestive of "jets", extending about 2″ (890 pc) to north and south. The map at 3.6 cm is similar to that at 6 cm and is not shown. The 20 cm map (Fig. 1) suggests that the fainter radio emission near the ends of the jet-like features bends eastward at the northern end of the source and westward at the southern end, giving the source an overall inverted "S"-shaped morphology.

The spectrum of the nuclear source between 20 and 6 cm is quite flat ($\alpha_{20-6}=0.22$, see Table 1) and appears to steepen at shorter wavelengths. Both sets of observations imply $\alpha_{20-6}<0.3$. Perhaps the nuclear core source is becoming optically thick to synchrotron self-absorption around 6 cm. The off-nuclear source shows a steeper spectrum characteristic of optically thin synchrotron radiation.

We believe that the off-nuclear source is likely to be associated with NGC 5252 rather than being an unrelated background source. First, the *a posteriori* chance of finding a

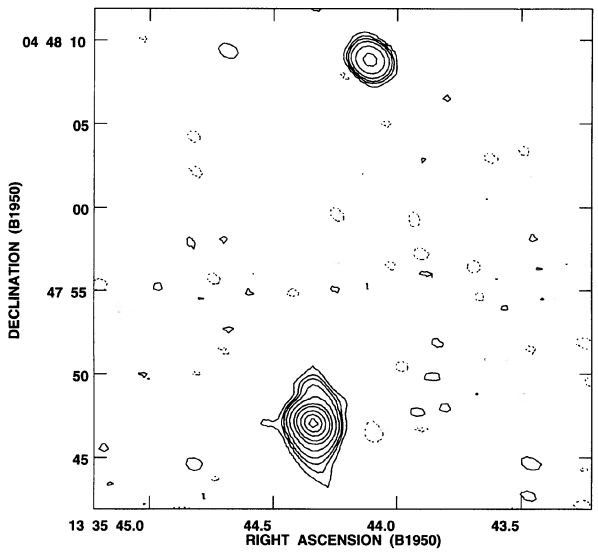

FIG. 1. Map of NGC 5252 at 20 cm wavelength. The southern source coincides with the optical nucleus. Contours are plotted at −1%, 1%, 2%, 3%, 5%, 10%, 20%, 30%, 50%, 70%, and 90% of the peak brightness of 11.1 mJy (beam area)$^{-1}$. The beam size is 1.55×1.27″ in PA 56°.

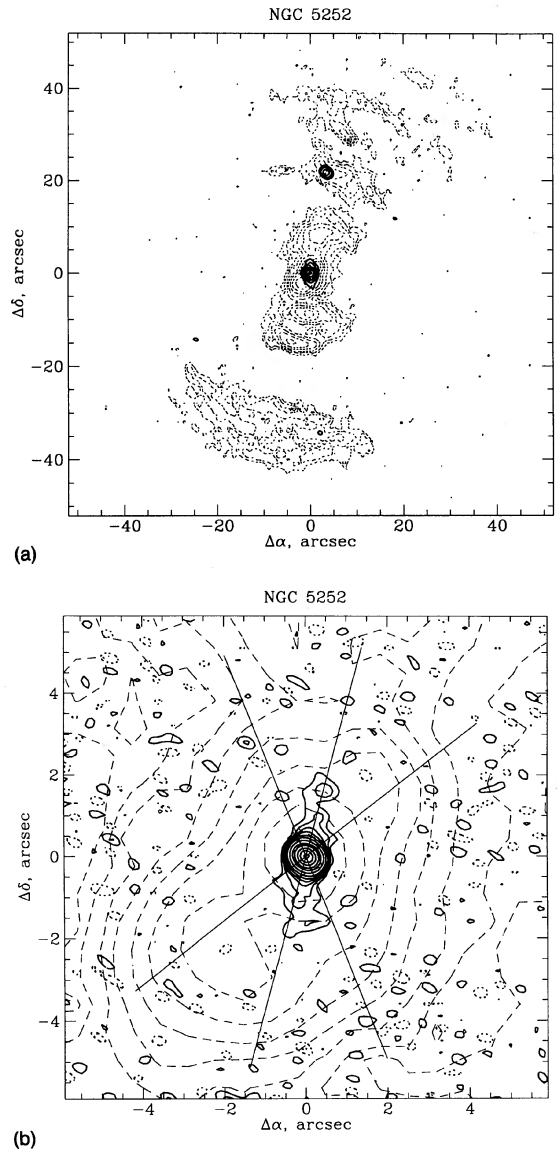

FIG. 2. Radio contours (solid lines) of NGC 5252 superposed on the [O III] λ5007 emission-line image (dashed lines) from Tadhunter & Tsvetanov (1989). (a) 20 cm radio map from Fig. 1; contours are plotted at 1.5%, 5%, 15%, 45%, and 90% of the peak brightness of 11.1 mJy (beam area)$^{-1}$. [O III] λ5007 contours are plotted at $3\sigma\times2''$, where σ is the noise and $n=0$, 1,...,8. The elongation of the nuclear source and the direction to the off-nuclear source are both approximately aligned with the ionization cone axis. Note the association of the off-nuclear source with one of the regions of emission-line gas. (b) 6 cm radio map. Radio contours are plotted at −1%, −0.5%, 0.5%, 1%, 1.5%, 2%, 3%, 5%, 10%, 20%, 30%, 50%, 70%, and 90% of the peak brightness of 9.9 mJy (beam area)$^{-1}$. The beam size is $0.46''\times0.38''$ in PA 58°. [O III] contours are the same as in (a). The three straight lines indicate the edges and axis of the larger scale ionization cones [see (a)]. Note the alignment of the radio source with the cone's axis.

background source of flux 1.9 mJy at 6 cm within 22″ of the nucleus of NGC 5252 is only ≃0.002 (using the source counts of Fomalont *et al.* 1991). Second, the source lies close to the extension of the radio axis of the nuclear source (see below), suggesting it is a product of the nuclear activity. Third, the off-nuclear radio source coincides with a region of emission-line gas in NGC 5252 (Figs. 2(a) and 3), as is commonly the case in Seyfert galaxies (e.g., Haniff *et al.* 1988); the radio emission may thus result from interaction between nuclear ejecta (an unseen jet?) and the interstellar medium. The absence of variability in the off-nuclear source between the two sets of radio observations (separated by 3 yr) argues that this source is not a supernova.

A summary of the directions on the sky of various features in NGC 5252 is given in Table 2. The position angle of the nuclear radio source was measured as close to the nucleus as possible from the 6 and 3.6 cm maps. It is clear that the axis of the nuclear radio source on the N side of the nucleus is aligned with that of the emission-line "ionization cone" to within the accuracy of the measurements. The nuclear radio emission on the S side of the nucleus and the off-nuclear radio source are both slightly misaligned with the emission-line cone axis, by 12°±6° and 6°±3°, respectively. The minor axis of the stellar distribution is inclined by some 60°–70° from both the radio and cone axes (cf. Fig. 3).

4. IONIZATION CONES IN SEYFERT GALAXIES

In the previous section, we noted the close correspondence between the radio and ionization cone axes of NGC 5252, and the large difference between these directions and the photometric minor axis of the galaxy. It is then of interest to check whether similar relationships apply to other Seyfert galaxies, as we now discuss.

4.1 Sample Selection

Unfortunately, there is no well-defined sample of ionization cones. The galaxies observed in emission-line imaging surveys of Seyfert galaxies generally do not comprise a complete sample. Further, if Seyfert nuclei are surrounded by dusty tori with columns up to 10^{24-25} cm^{-2} (e.g., Mulchaey *et al.* 1992), all samples are potentially subject to orientation dependent selection effects. Lastly, the definition of an ionization cone, although clear in principle, is difficult to quantify. In some cases, sharp-edged bi-cones with a common nuclear apex are immediately obvious and striking (e.g., NGC 5252, Tadhunter & Tsvetanov 1989; NGC 5728, Wilson *et al.* 1993). In other cases, the emission-line gas may be quite compact and/or the cone may be seen on only one side of the nucleus. Here the interpretation of the morphology in terms of a collimated ionizing source is less compelling. Bearing in mind these caveats, we have compiled a list of ionization cones from the literature. Because of the problems discussed above, our conclusions concerning the alignments between the cones and other axes of the galaxies should be considered tentative.

4.2 Relative Orientation of the Ionization Cone, Nuclear Radio, and Galactic Minor Axes

Table 3 gives a list of position angles and opening angles for Seyfert galaxies with ionization cones. The columns list the galaxy name (column 1), the PA of the radio axis (column 2), the approximate spatial scale (i.e., the radial distance from the nucleus) on which the radio axis was measured (column 3), the PA of the ionization cone axis (column 4),

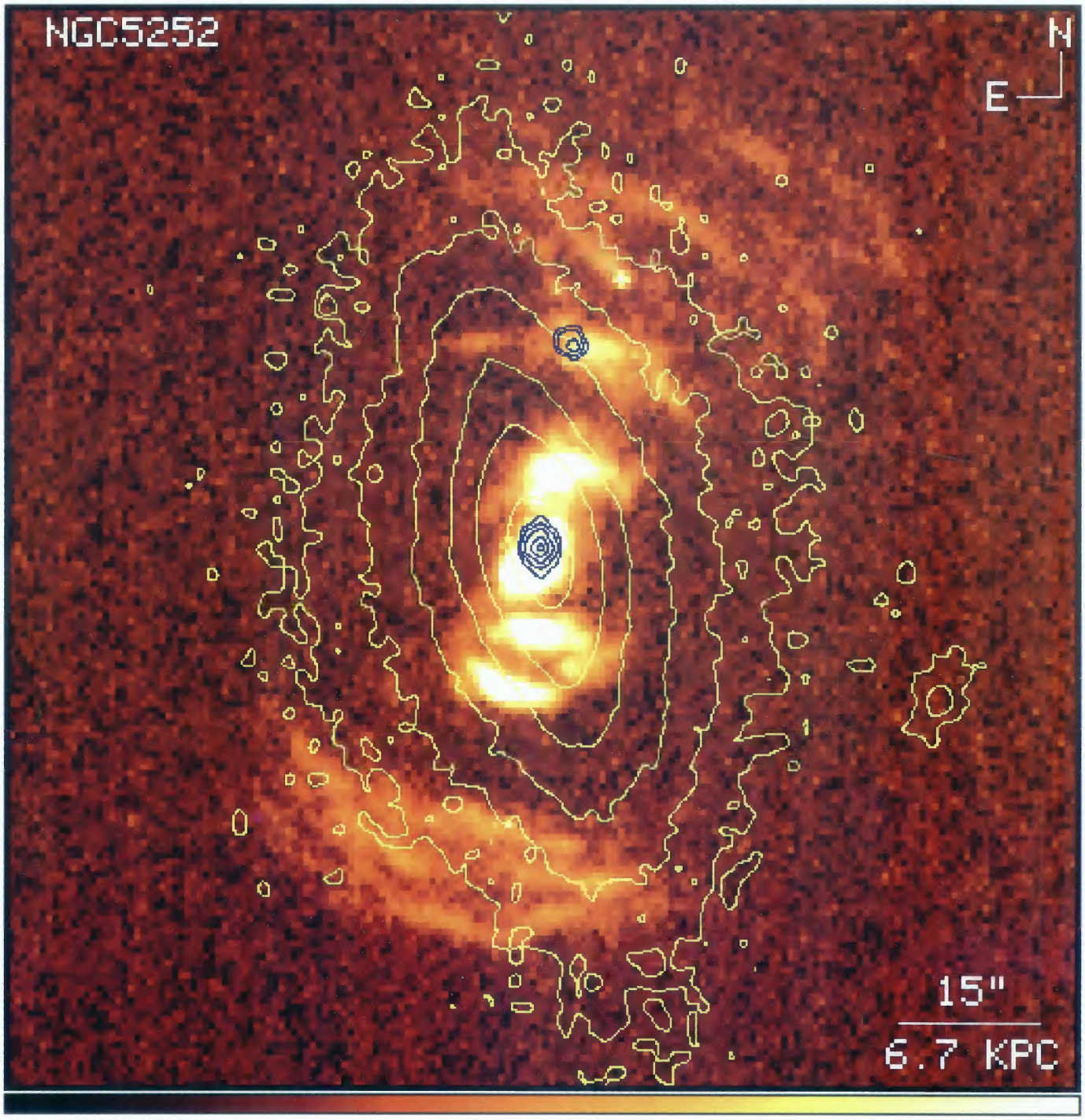

FIG. 3. The color picture is the [O III] λ5007 image from Tadhunter & Tsvetanov (1989). The yellow contours represent the green continuum emission (center wavelength 5210 Å, width ≈60 Å), also from Tadhunter & Tsvetanov (1989). Contours are plotted at 0.3%, 0.6%, 1.2%, 2.5%, 5%, 15%, 45%, and 90% of the peak. The blue contours are the VLA 20 cm radio map, with contours at 1.5%, 5%, 15%, 45%, and 90% of the peak value.

the approximate spatial scale (i.e., the radial distance from the nucleus) on which the ionization cone axis was measured (column 5), the PA of the minor axis of the galaxy disk (column 6), the opening angle of the radio emission measured at the nucleus (column 7), and the opening angle of the ionization cone measured at the nucleus (column 8). The radio axis was measured as close as possible to the nucleus from the highest resolution map available, unless otherwise stated. The direction of the minor axis refers to the outer disk and is often a kinematic determination. The radio opening angle represents the most collimated radio component. When there are two cones, on opposite sides of the nucleus, the relevant numbers are listed separately. The opening angle of the ionization cones is a somewhat subjective parameter and may depend on the nuclear distance at which it is measured. Table 4 contains the galaxy name (column 1), its morphological type (column 2), the difference between the position angles of the radio and ionization cone axes (column 3), and

TABLE 2. Directions in NGC 5252[1].

Feature (1)	Position angle (°) (2)
Nuclear radio source	345 ± 3 (N side), 175 ± 5 (S side)
Off-nuclear source (w.r.t. nucleus)	351.09 ± 0.02
Axis of emission-line cone	345 ± 3 (N side), 163 ± 3 (S side)
Major axis of stellar disk	12.5 ± 2

Note to TABLE 2

[1]1950.0 coordinate system.

the difference between the position angles of the minor axis of the galaxy disk and the ionization cone axis (column 4).

It is immediately apparent from column 3 of Table 4 that there is a tight correlation between the radio and ionization cone axes. A similar relationship was noted by Pogge (1989) from a smaller sample. These axes are aligned to within the errors for almost all galaxies: the formal mean difference between the measured radio and cone axes is only 6° and this number can be taken as an upper limit to the typical difference between the preferred directions of escape from the nucleus of the radio plasma and ionizing photons. The good alignment between the radio and ionization cone axes indicates that bending of the trajectories of the radio lobes by buoyancy (e.g., Hummel *et al.* 1983) is unimportant on the small spatial scales on which the radio position angles were measured.

In NGC 1068, it is notable that the axes of both the radio ejecta and the ionization cones change with increasing distance from the nucleus, while maintaining a close correspondence with each other. This result suggests that both the radio plasmoid and ionizing photon trajectories are recollimated on the ≃100 pc scale. Presumably this recollimation is effected by a gaseous torus, the plane of which warps by ≃15° between the <30 pc and ≃100 pc scales.

For the sample as a whole, there is no strong correlation between the galactic minor and ionization cone axes. Such would be expected given the known lack of correlation between the radio and galactic minor axes in Seyferts (Ulvestad & Wilson 1984b) and the above described tight relation between the radio and ionization cone axes. If, however, the difference between the galactic minor and ionization cone axes is considered as a function of galaxy morphological type, an interesting possible trend emerges (Fig. 4). The difference between minor and ionization cone axes tends to be large for early-type galaxies and smaller for late-type ones. The formal probability of no correlation in Fig. 4 is <0.1%. This significance level is sensitive to the very uncertain morphological type of Mkn 78. It is noteworthy that in the case of NGC 1068 (type Sb), the smaller the scale, the closer the

TABLE 3. Ionization cones and radio sources: Directions and opening angles.[1]

Galaxy (1)	PA radio (°) (2)	Scale of radio (pc) (3)	PA ioniz'n cone (°) (4)	Scale of ioniz'n cone (pc) (5)	PA minor axis (°) (6)	Radio opening angle (°) (7)	Ioniz'n cone opening angle (°) (8)
NGC 1068[2]	33 ± 2	140	32 ± 5	120–350	170 ± 9	<30	40 ± 10
	20 ± 5	40	15 ± 5	20–70		<10	65 ± 20
NGC 1365	-	-	135 ± 10	210–800	138 ± 10	-	(102 ± 20)
NGC 3281	-	-	25 ± 10	550–1300	47 ± 3	-	75 ± 10
NGC 4151	57 ± 5	1	60 ± 5 (NE)	15–70 (NE)	116 ± 3	<5	67 ± 10 (NE)
	-	-	240 ± 5 (SW)	15–80 (SW)			75 ± 10 (SW)
NGC 4388	26 ± 5 (N)	150 (N)	≈35 (N)	2200 (N)	0 ± 3	<12	≈50 (N)
	199 ± 2 (S)	150 (S)	193 ± 5 (S)	180–900 (S)			92 ± 7 (S)
NGC 5252	345 ± 3 (N)	760 (N)	345 ± 3 (N)	3600–18000 (N)	102.5 ± 3	<0.3	74 ± 3 (N)
	175 ± 5 (S)	670 (S)	163 ± 3 (S)	6700–18000 (S)			73 ± 3 (S)
NGC 5728	307 ± 4 (NW)	590 (NW)	304 ± 5 (NW)	70–270 (NW)	88.5 ± 1	≈20	60 ± 10 (NW)
	-	-	118 ± 5 (SE)	90–1200 (SE)			56 ± 10 (SE)
NGC 7582	-	-	244 ± 5	200–760	75 ± 10	-	86 ± 10
Mkn 6	357 ± 3	200	345 ± 10	≈3600	40 ± 7	<15	–
Mkn 78	270 ± 4	720	262 ± 5	8600	174 ± 4	≈25	50 ± 10
Mkn 573	308 ± 5 (NW)	400 (NW)	300 ± 5 (NW)	670–1300 (NW)	(160 ± 25)	<30	45 ± 10 (NW)
	118 ± 4 (SE)	530 (SE)	120 ± 5 (SE)	670–1700 (SE)			45 ± 10 (SE)

Notes to TABLE 3

[1]References for the information listed are as follows:
NGC 1068: Wilson & Ulvestad (1987), Ulvestad *et al.* (1987), Pogge (1988a), Evans *et al.* (1991), and Baldwin *et al.* (1987).
NGC 1365: Storchi-Bergmann & Bonatto (1991), and Phillips *et al.* (1983).
NGC 3281: Storchi-Bergmann *et al.* (1992).
NGC 4151: Harrison *et al.* (1986), Evans *et al.* (1993), Davies (1973), and Simkin (1975).
NGC 4388: Hummel & Saikia (1991), Pogge (1988b, 1989), and Corbin *et al.* (1988).
NGC 5252: This paper, and Tadhunter & Tsvetanov (1989).
NGC 5728: Schommer *et al.* (1987), and Wilson *et al.* (1993).
NGC 7582: Storchi-Bergmann & Bonatto (1991), unpublished observations by H. B. Kirkpatrick, and Morris *et al.* (1985).
Mkn 6: Ulvestad & Wilson (1984a), and Meaburn *et al.* (1989).
Mkn 78: Pedlar *et al.* (1989), and Haniff *et al.* (1988).
Mkn 573: Ulvestad & Wilson (1984a), Haniff *et al.* (1991), and Tsvetanov & Walsh (1992).
[2]For NGC 1068, the two lines give the radio and ionization cone properties on two different spatial scales.

TABLE 4. Alignments of ionization cones, radio sources, and minor axes.[1]

Galaxy (1)	Morphological Type (2)	PA Radio minus PA Ioniz'n Cone (°) (3)	PA Minor Axis minus PA Ioniz'n Cone (°) (4)
NGC 1068[2]	(R)S(rs)b	+ 1 ± 5	− 42 ± 10
		+ 5 ± 7	− 25 ± 10
NGC 1365	SB(s)b	-	+ 3 ± 14
NGC 3281	S(s)abpec:	-	+ 22 ± 10
NGC 4151	(R')SAB(rs)ab:	− 3 ± 7	+ 56 ± 6 (NE)
			+ 56 ± 6 (SW)
NGC 4388	S(s)b:sp	≈− 9 (N)	≈− 35 (N)
		+ 6 ± 5 (S)	− 13 ± 6 (S)
NGC 5252	S0	0 ± 4 (N)	− 63 ± 4 (N)
		+ 12 ± 6 (S)	− 61 ± 4 (S)
NGC 5728	SAB(r)a:	− 4 ± 6 (NW)	− 36 ± 5 (NW)
		-	− 29 ± 5 (SE)
NGC 7582	(R')SB(s)ab	-	− 11 ± 11
Mkn 6	SAB0$^+$:	+ 12 ± 10	+ 55 ± 12
Mkn 78	S0:, E:,	+8±6	−88±6
Mkn 573	(R)SABO$^+$(rs):	+ 8 ± 7 (NW)	(+ 40 ± 25) (NW)
		− 2 ± 6 (SE)	(+ 40 ± 25) (SE)

Notes to TABLE 4

[1]Morphological types are from de Vaucouleurs *et al.* (1991) except for Mkn 78 which was estimated by the present authors.

[2]For NGC 1068, the upper numbers refer to the 6″ (440 pc) scale and the lower to the 0.5″–1″ (35–70 pc) scale.

radio and ionization cone axes align with the projected galaxy disk rotation axis.

5. DISCUSSION

5.1 The Relationship between Ionization Cones and Radio Ejecta

Although the sample is both limited in size and incomplete, our study demonstrates a remarkably tight correlation between radio source and ionization cone axes in Seyfert galaxies. This result indicates that the ejection of radio components and the escape of ionizing photons are collimated by the same, or coplanar, disks. It is also clear from Table 3 that the *degree* of collimation is much better for the radio plasma than for the ionizing photons.

Ionization cones may result from collimation at the source of emission of the ionizing photons or by absorption of an intrinsically isotropic source. Mechanisms expected to provide collimation in emission include thermal radiation from the funnel of a radiation torus (e.g., Madau 1988) and beaming by a mildly relativistic jet. Collimation by absorption is usually ascribed to shadowing by a dusty molecular torus (Antonucci & Miller 1985; Krolik & Begelman 1988). Powerful radio jets are thought to arise through electromagnetic effects associated with accretion disks or spinning black holes (e.g., Blandford 1990). Alternatively, the relatively weak radio jet-like structures in Seyferts might arise through acceleration by radiation pressure in the funnel of an accretion torus (e.g., Abramowicz & Piran 1980; Ghisellini *et al.* 1990).

The key issue is whether the radio plasma and ionizing photons are collimated on the same or different spatial scales. The most stringent limit on the collimation of radio ejecta in Seyferts is provided by VLBI observations of NGC 4151 (Harrison *et al.* 1986), which show that the collimation occurs on a scale <2 pc. *HST* observations of NGC 1068 (Evans *et al.* 1991), NGC 4151 (Evans *et al.* 1993), and NGC 5728 (Wilson *et al.* 1993) indicate that the ionization cones are formed <20 pc from the nucleus. Both emission and absorption models of the collimation of the ionizing pho-

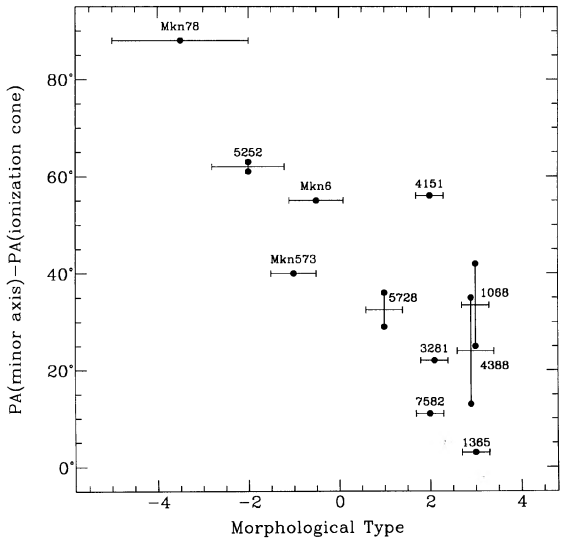

FIG. 4. Orientation of the galactic minor axis with respect to the ionization cone axis plotted as a function of the morphological type of the galaxy. Vertical lines connect the values for two cones in a given galaxy on opposite sides of the nucleus, except for NGC 1068 where they connect the values for the cones to the NE of the nucleus on different spatial scales (see Table 4). The morphological types (and errors) are taken from de Vaucouleurs *et al.* (1991), except for Mkn 78 which was estimated by the present authors. Each object is indicated by its NGC or Markarian number. For clarity, the vertical bar for NGC 4388 is slightly offset from its nominal position.

tons are consistent with this observational limit.

Current observations do not allow a choice to be made between these various possible origins for the ionization cones and radio ejecta. We therefore restrict our discussion to two consequences of our empirical results.

5.1.1 Channel cleared by radio jet

It is possible that the ionization cone–radio ejecta alignment represents a direct cause and effect relationship. In one scenario (e.g., Schulz 1988), the nucleus is surrounded by a cloud which is initially opaque to ionizing radiation in all directions. A radio jet turns on, plows through the cloud, and opens up a low density channel through which ionizing radiation can escape. In such a model, the two axes would be naturally coaligned.

We have shown that the radio ejecta are much better collimated than the ionizing photons (Table 3). This result is at adds with the simplest geometry, in which the radio jet scours a long, narrow channel through the cloud, and the source of ionizing photons is located at the nucleus and is small compared with the radial extent of the cloud. The large opening angles of the ionization cones require that the diameter of the hole be comparable to its length. One obvious solution is to postulate that the high velocity, narrow jet represents only the core of a slower, wide angle gaseous outflow, and the latter clears a much larger hole in the gas cloud. Optical observations provide clear evidence for such wide-angle, gaseous outflows from Seyfert galaxies (e.g., Wilson 1993).

5.1.2 Limits on disk precession

If the radio jets originate from the accretion disk (scale $<10^{16}$ cm) around the central black hole, and the ionization cones result from shadowing by a much larger, dusty torus (scale $>10^{18}$ cm, see below), our results show that the two structures are accurately coaligned. This alignment restricts any precession of the orbiting gas as it is accreted from the larger to the smaller scales, as we now discuss. Dust sublimes at temperatures $T_{\rm eff}>2000$ K and the corresponding radius of the inner edge of the dusty torus is $r_{\rm i}\simeq 0.015 L_{44}^{1/2}(T_{\rm eff}/2000\ {\rm K})^{-2}(Q_{\rm a}/Q_{\rm e})^{1/2}$ pc, where L_{44} is the central luminosity in units of 10^{44} erg s^{-1}, and $Q_{\rm a}/Q_{\rm e}$ is the ratio of the optical absorption coefficient to the infrared emission coefficient. For $L_{44}\simeq 10$ and $Q_{\rm a}/Q_{\rm e}\simeq 100$, $r_{\rm i}\simeq 0.5$ pc. In a more sophisticated analysis, Krolik & Begelman (1988) have argued that the inner edge of the torus is determined by the balance between the inward mass flow of clouds and the rate at which the nuclear continuum can evaporate them. With a number of assumptions, they estimate $r_{\rm i}\simeq L_{44}(L/L_{\rm E})^{-3}(T_{\rm c}/3\times 10^7\ {\rm K})^{-2}$ pc, where $L_{\rm E}$ is the Eddington luminosity and $T_{\rm c}$ the Compton temperature. Both arguments indicate that the inner edge of the torus is expected to be pc-scale or larger for luminous Seyferts. Unless the angular momentum of the orbiting gas aligns with the axis of symmetry of the mass distribution, the torus will precess about the axis of symmetry on a times scale $\tau_{\rm p}\approx\omega^{-1}J_2^{-1}$ (e.g., Tohline *et al.* 1982), where ω is the angular velocity of the gas particle and J_2 is the coefficient of the quadrupole moment of the gravitational field (this formula assumes J_2 is small and the radius of the gravitating body is smaller than the particle radius). In order to maintain the inner disk–dusty torus alignment, either

(i) the gravitational field is sufficiently spherically symmetric that $\tau_{\rm p}>>\tau_{\rm a}+\tau_{\rm d}$, where $\tau_{\rm a}$ is the accretion time scale from the torus to the disk, and $\tau_{\rm d}$ is the difference between the times taken for the radio ejecta and ionizing photons to propagate from the nucleus to their observed scales ($\tau_{\rm d}\simeq r_{\rm r}/v_{\rm r}-r_{\rm i}/{\rm c}$, where $r_{\rm r}$ and $v_{\rm r}$ are the radius and outward velocity of the radio components, $r_{\rm i}$ is the radius of the ionization cone, and c is the speed of light), or

(ii) the dusty torus has already settled into one of the principal planes of the mass distribution.

A spherically symmetric gravitational field at the dusty torus would be assured if the nuclear black hole dominates the stellar potential there. Assuming that the nonpoint mass contribution to the gravitational potential is the same as in our galaxy, the central black hole dominates the potential inside the radius $r_{\rm bh}\simeq 10(L_{\rm E}/L)L_{44}$ pc (Krolik & Begelman 1988). It is thus plausible that the gravitational potential at the dusty torus is close to being spherically symmetric.

5.2 The Relationship between Ionization Cone and Galactic Disk Axes

We have also found a possible trend for the known ionization cones to align with the rotation axis of the galaxy disk for late-type galaxies but not for early-types (Fig. 4). There are two possible explanations:

(i) The trend is a selection effect. Ionization cones are most easily recognized when the high excitation gas in the cone is not projected against the H II regions of a galaxy disk. Thus we expect cones in late-type galaxies to be most readily seen when they align perpendicular to a disk viewed close to edge-on. Indeed, three of the galaxies (NGC 3281, 4388, and 7582) with types equal to or later than Sab (i.e., $T\geqslant 2$) are highly inclined. This selection effect is presumably less important for early-type systems where H II regions are less prominent.

(ii) The trend could be real, implying that the inner gas disks responsible for collimating the escape of ionizing photons in late-type Seyferts tend to align with the host galaxy disk, while those in early-type ones do not. The inner gas disks are probably accreted from the galaxy-scale gaseous medium (e.g., Krolik & Begelman 1988). In late-type systems, this galaxy-scale gas disk is associated with the stellar disk, but in early-type galaxies it may not be (e.g., Knapp *et al.* 1985). The gas in the early-type systems may have an origin external to the galaxy, such as through accretion from a companion (e.g., Knapp *et al.* 1985; Wardle & Knapp 1986). In this way, the axis of the circumnuclear disk would depend on the nature and origin of the galaxy-scale gaseous distribution.

We thank NRAO for hospitality during the processing of the VLA data, G. van Moorsel for obtaining the second set of radio observations of NGC 5252 and the referee for helpful comments. This research was supported by NASA Grants NAGW-2689, NAGW-3268, and NAG8-793.

REFERENCES

Abramowicz, M. A., & Piran, T. 1980, ApJ, 241, L7
Antonucci, R. R. J., & Miller, J. S. 1985, ApJ, 297, 621
Antonucci, R. R. J., 1993, ARA&A, 31, 473
Argyle, R. W., & Eldridge, P. 1990, MNRAS, 243, 504
Argyle, R. W. 1993, private communication
Baldwin, J. A., Wilson, A. S., & Whittle, M. 1987, ApJ, 319, 84
Blandford, R. D. 1990, in Active Galactic Nuclei, R. D. Blandford, H. Netzer, & L. Woltjer, SAAS-Fee Advanced Course 20, edited by T. J.-L. Courvoisier and M. Mayor (Springer, Berlin)
Corbin, M. A., Baldwin, J. A., & Wilson, A. S. 1988, ApJ, 334, 584
Davies, R. D. 1973, MNRAS, 161, 25P
de Vaucouleurs, G., de Vaucouleurs, A., Corwin, H. G., Jr., Buta, R. J., Paturel, G., & Fouqué, P. 1991, Third Reference Catalogue of Bright Galaxies (Springer, Berlin)
Evans, I. N., Ford, H. C., Kinney, A. L., Antonucci, R. R. J., Armus, L., & Caganoff, S. 1991, ApJ, 369, L27
Evans, I. N., Tsvetanov, Z., Kriss, G. A., Ford, H. C., Caganoff, S., & Koratkar, A. 1993, ApJ, 417, 82
Fomalont, E. B., Windhorst, R. A., Kristian, J. A., & Kellerman, K. I. 1991, AJ, 102, 1258
Ghisellini, G., Bodo, G., Trussoni, E., & Rees, M. J. 1990, ApJ, 362, L1
Haniff, C. A., Wilson, A. S., & Ward, M. J. 1988, ApJ, 334, 104
Haniff, C. A., Ward, M. J., & Wilson, A. S. 1991, ApJ, 368, 167
Harrison, B., Pedlar, A., Unger, S. W., Burgess, P., Graham, D. A., & Preuss, E. 1986, MNRAS, 218, 775
Hummel, E., van Gorkom, J. H., & Kotanyi, C. G. 1983, ApJ, 267, L5
Hummel, E., & Saikia, D. J. 1991, A&A, 249, 43
Knapp, G. R., van Driel, W., & van Woerden, H. 1985, A&A, 142, 1
Knapp, G. R., Turner, E. L., & Cunniffe, P. E. 1985, AJ, 90, 454
Krolik, J. H. & Begelman, M. C. 1988, ApJ, 329, 702
Meaburn, J., Whitehead, M. J., & Pedlar, A. 1989, MNRAS, 241, 1P
Morris, S. L., Ward, M. J., Whittle, D. M., Wilson, A. S., & Taylor, K. 1985, MNRAS, 216, 193
Mulchaey, J. S., Mushotzky, R. F., & Weaver, K. A. 1992, ApJ, 390, L69
Pedlar, A., Meaburn, J., Axon, D. J., Unger, S. W., Whittle, D. M., Meurs, E. J. A., Guerrine, N., & Ward, M. J. 1989, MNRAS, 238, 863
Phillips, M. M., Turtle, A. J., Edmunds, M. G., & Pagel, B. E. J. 1983, MNRAS, 203, 759
Pogge, R. W. 1988a, ApJ, 328, 519
Pogge, R. W. 1988b, ApJ, 332, 702
Pogge, R. W. 1989, ApJ, 345, 730
Schommer, R. A., Caldwell, N., Wilson, A. S., Baldwin, J. A., Phillips, M. M., Williams, T. B., & Turtle, A. J. 1988, ApJ, 324, 154
Schulz, H. 1988, A&A, 203, 233
Simkin, S. M. 1975, ApJ, 200, 567
Storchi-Bergmann, T., & Bonatto, C. J. 1991, MNRAS, 250, 138
Storchi-Bergmann, T., Wilson, A. S., & Baldwin, J. A. 1992, ApJ, 396, 45
Tadhunter, C. N., & Tsvetanov, Z. I. 1989, Nature, 341, 422
Tohline, J. E., Simonson, G. F., & Caldwell, N. 1982, ApJ, 252, 92
Tsvetanov, Z. I., & Walsh, J. R. 1992, ApJ, 386, 485
Ulvestad, J. S., & Wilson, A. S. 1984a, ApJ, 278, 544
Ulvestad, J. S., & Wilson, A. S. 1984b, ApJ, 285, 439
Ulvestad, J. S., Neff, S. G., & Wilson, A. S. 1987, AJ, 93, 22
Unger, S. W., Pedlar, A., Axon, D. J., Whittle, M., Meurs, E. J. A., & Ward, M. J. 1987, MNRAS, 228, 671
Wardle, M., & Knapp, G. R. 1986, AJ, 91, 23
Whittle, M., Pedlar, A., Meurs, E. J. A., Unger, S. W., Axon, D. J., & Ward, M. J. 1988, ApJ, 326, 125
Wilson, A. S. 1993, in Astrophysical Jets, STScI Symp. Series No. 6, edited by D. Burgarella, M. Livio, and C. P. O'Dea (Cambridge University Press), p. 121
Wilson, A. S., & Ulvestad, J. S. 1987, ApJ, 319, 105
Wilson, A. S., Braatz, J. A., Heckman, T. M., Krolik, J. H., & Miley, G. K. 1993, ApJ, 419, L61